** For BSSA — V. 1.7: 12/26/03 **

A Study of Possible Ground-Motion Amplification at the Coyote Lake Dam, California

by David M. Boore, Vladimir M. Graizer, John C. Tinsley, and Anthony F. Shakal

Abstract

The abutment site at the Coyote Lake Dam recorded an unusually large peak acceleration of 1.29g during the 1984 Morgan Hill earthquake. Following this earthquake another strong-motion station was installed about 700 m downstream from the abutment station. We study all events (7) recorded on these stations, using ratios of peak accelerations, spectral ratios, and particle motion polarization (using hodograms) to investigate the relative ground motion at the two sites. We find that in all but one case the motion at the abutment site is larger than the downstream site over a broad frequency band. The polarizations are similar for the two sites for a given event, but can vary from one event to another. This suggests that the dam itself is not strongly influencing the records. Although we can be sure that the relative motion is usually larger at the abutment site, we cannot conclude that there is anomalous site amplification at the abutment site. The downstream site could have lower than usual near-surface amplifications. On the other hand, the geology near the abutment site is extremely complex and includes fault slivers, with rapid lateral changes in materials and presumably seismic velocities. For this reason alone, the abutment site should not be considered a "normal" free-field site.

Introduction

During the 1984 Morgan Hill, California, earthquake, a station adjacent to the Coyote Lake Dam in California (Figure 1) recorded a horizontal peak acceleration of 1.29g (Shakal *et al.*, 1984a). This is one of the highest peak accelerations measured for the horizontal component of earthquake-induced ground shaking at the Earth's surface,

exceeded only by four other recordings (according to a search on the COSMOS web site (http://db.cosmos-eq.org/), which yielded the following larger recordings: Station 1, 1985 Nahanni; Cape Mendocino, 1992 Cape Mendocino; Tarzana, 1994 Northridge; Pacoima Dam, 1994 Northridge). A map of the region around Coyote Lake Dam is shown in Figure 1, and Figure 2 displays the acceleration time series recorded during the 1984 Morgan Hill earthquake. As the rupture in the earthquake headed directly toward the station, one explanation of the large acceleration is that its amplitude has been increased owing to directivity (e.g., Niazi, 1984). On the other hand, the earthquake was composed of two dominant subsources (e.g., Bakun *et al.*, 1984; Uhrhammer and Darragh, 1984; Hartzell and Heaton, 1986; Beroza and Spudich, 1988), and another interpretation is that the large amplitude is due to the constructive interference between the S-waves from the first subsource and the closer second subsource, with directivity playing only a minor role (Abrahamson and Darragh, 1985). None of the studies just mentioned considered site response as a cause of the large motions. The possibility that the high ground motions were very localized was raised by Hovland *et al.* (1984) as a result of their survey of damage in the vicinity of the Coyote Lake Dam. Noting the lack of damage to concrete block and brick buildings and walls, as well as small storage tanks, all within 4 km of the dam, and the few rockfalls in the vicinity of the dam, they inferred that either:

> "1. The high peak ground accelerations recorded by [the abutment] instrument reflect a very localized behavior or response, or that"

> "2. Rather ordinary structures and earth dams can survive ground motions involving peak accelerations well over 1.0g with little or no damage."

They did not say which possibility they prefer, but we suspect it was item 1. On the other hand, Shakal *et al.* (1984b) point out that the abutment site recorded a peak acceleration of 0.25g during the 1979 Gilroy earthquake; none of the studies using that record to model the rupture process in the 1979 earthquake questioned the amplitude of the recording at the abutment station (e.g., Bouchon, 1982; Liu and Helmberger, 1983). The peak acceleration at the abutment station for the 1979 Gilroy earthquake is not unusual; it falls between those given by two commonly-used empirical ground-motion predictions equations: 0.18g (Boore *et al.*, 1997) and 0.34g (Abrahamson and Silva, 1997).

To address the possibility that there could be unusual site response associated

with the abutment site, following the 1984 earthquake the California Strong-Motion Instrumentation Program of the California Geological Survey installed another instrument about 700 m downstream from the instrument at the dam (the instruments at both sites are analog-recording accelerometers). Five events, three of which produced motions large enough to digitize (one of the events was the 1989 **M** 6.9 Loma Prieta earthquake), have now been recorded at both the abutment and the downstream sites. In this article we use all of the recordings at the two stations to study the relevant differences at the two sites. In all but one noteworthy case (Graizer *et al.*, 2002), the motions at the dam site are larger than those at the downstream site for a wide range of frequencies. Polarization diagrams (hodograms) are generally consistent for both the abutment and the downstream stations, and are earthquake specific, suggesting that the dam response is not influencing the response to a significant extent.

Description of Stations

The abutment station (Figure 3) is located on the southwest side of an earth dam placed across a valley in the Calaveras fault zone (Figure 4). The dam "is one of the few in the US knowingly built across an active fault" (Tepel *et al.*, 1984). Completed in 1936, it was designed to withstand horizontal and vertical displacements of 4.6 m and 1.5 m, respectively, without catastrophic release of water. The dam has an impervious clay core, covered with coarse gravel intended to fill any cracks in the clay core, and this is covered with boulder rip-rap to provide a driving force to fill the cracks. The abutment instrument is located very close to a large knob of silica-carbonate and serpentine, and this resistant knob is embedded in sheared rocks of the Franciscan assemblage (Fumal *et al.*, 1987). The geology in the region is well-known from exploratory drilling and tunnels made before dam construction (the exploratory tunnels, one of which goes below the knob of rock, have been filled with grout). Figure 5 shows contours before and after dam construction, and from this it is clear that prior to dam construction, the knob of rock was a prominent cut-off spur of a ridge; there seems to be up to about 1.5 m of fill beneath the abutment station. What is not known are the relative seismic velocities of the rock comprising the knob and the material used in constructing the dam. Velocities were obtained in a 30-m deep borehole only 70 m from the strong-motion station, but that borehole penetrated only sedimentary rocks, rocks that are much younger than the rocks comprising the knob near the station (Fumal *et al.*, 1987). A strand of the Calaveras fault separates the rocks

at the borehole site from those near the strong-motion station. For this reason, the seismic velocities measured from the borehole are not representative of those at the strong-motion site.

In contrast, the downstream site is in a region of less complex geology, at least near the site itself (Figures 3 and 4). The site was chosen after the 1984 event by one of us (AFS), working with others, to provide a reference site with relatively flat-lying topography and simple geology, well removed from the possible influence of the dam itself. The site is just outside and to the east of the Calaveras fault zone, on a bouldery slope of colluvium with the ground surface sloping at about 10 degrees. The colluvial deposit seems to be poorly sorted and has a number of boulders at the surface. The colluvium is underlain by Cretaceous rocks of the Great Valley Sequence (Wentworth *et al.*, 1998). No shear-wave velocities have been measured at or near the site.

The recorders at both stations were triggered, film-recording accelerographs at the time of the recordings studied here. The coordinates of the stations are given in Table 1.

Data Used in the Study

Seven earthquakes have been recorded at the abutment station, starting with the 1979 Coyote Lake earthquake. Five of these events were also recorded at the downstream station, and three produced motions large enough to be worthy of digitizing. Earthquake information is given in Table 2, and the epicenters (and approximations of the rupture surfaces for the three largest earthquakes) are shown in Figure 1. All but the 1989 Loma Prieta earthquake and the small earthquake of 2002 occurred along the Calaveras fault zone. The table also includes the largest peak horizontal acceleration recorded at each station, as well as the ratio of the peak accelerations at the abutment and downstream sites (the stations are so close relative to the hypocentral distances that no corrections were made for differences in geometrical spreading). Note that for all except one event the ratio is larger than unity. In subsequent sections we look into this in more detail for the five events for which digital data are available (the peak accelerations for the non-digitized recordings were scaled from the film records).

Time series for the three events providing digitizable data at both the abutment and downstream sites are shown in Figures 6, 7, and 8. Figure 6 shows the acceleration,

velocity, and displacement time series for horizontal motion in the direction of maximum polarization (305°, as determined in the next section), which is close to being in the fault-parallel direction (326°), from the 1989 Loma Prieta earthquake. The data for the other two events have been rotated into fault normal and fault parallel directions. Note that the abutment and downstream motions are similar in shape and amplitude for the long periods in the 1989 ground displacements, but that the correlation starts to break down after the first arrival for higher frequencies (as shown by the velocity and acceleration traces for the 1989 event and for all traces for the 1993/08/11 earthquake); for these two events the abutment motion is generally larger than the downstream motion. In distinct contrast is the motion from the 1993/01/16 earthquake (Figure 7). The motion is almost perfectly polarized in the fault-normal direction, and the downstream motion is somewhat larger than the abutment for the displacement, velocity, and acceleration traces.

Hodograms of Horizontal Motion

Particle motion plots ("hodograms") are a compact way of seeing information about the ground motion. These plots have been constructed for all of the digitized data available to use from the abutment and the downstream stations, and are shown in Figures 9 through 12. Hodograms are shown for the acceleration, velocity, and displacement traces. Only the time segment surrounding the dominant motion was used in making the plots.

The hodograms for the 1979, 1984, and 1989 earthquakes all show a dominant polarization oriented approximately 50 to 60 degrees west of north. This polarization exists on the acceleration, velocity, and displacement traces, and on both the abutment and the downstream station for the 1989 earthquake (recall that the downstream station was installed following the 1984 earthquake). The strike of the Calaveras fault zone is approximately 326 to 330 degrees. Thus the dominant polarization of the ground motion is closer to fault parallel than to fault normal. The 1979 and 1984 earthquakes were almost pure strikeslip events, and we would expect that the largest horizontal ground motions would have an orientation perpendicular to the fault. This discrepancy was noted by Beroza and Spudich (1988); they invoked lateral changes in the crustal velocity as an explanation for the discrepancy.

In distinct contrast to the motions from the 1979, 1984, and 1989 earthquakes, the hodograms for the two 1993 earthquakes show an orientation that are consistent with being

fault normal (more so for the 09/16 event than for the 08/11 event). As the locations of these two earthquakes were along the Calaveras fault (Figure 1), with the hypocenter of the 1993/08/11 event being almost co-located with that of the 1984 earthquake, it is hard to understand why there would be a difference in the polarizations between the 1993 earthquakes and the 1979 and 1984 earthquakes. The consistent difference in the particle motions pre- and post-1992 makes one wonder whether the data have been mislabeled. We checked the original data and the station service records, and are convinced that the components are correctly labeled.

We did note an interesting apparent 90 degree change in the polarization of the horizontal motion for the two 1993 events at the abutment station, as shown in Figures 11 and 12 by differing line widths for consecutive 1.5 to 2 sec time windows. The larger, earlier motion is oriented almost perpendicular to the fault, but that motion is followed by smaller motion with an orientation similar to that seen in the 1979, 1984, and 1989 events. Some authors (e.g., Bonamassa and Vidale, 1991; Vidale *et al.*, 1991; Spudich *et al.*, 1996) have found that ground-motion polarization can be a site characteristic, independent of the azimuth to the source. The consistency of the polarizations between the abutment and the downstream stations, and the change in the polarizations for the earlier and the later events argues against this being the case here.

The hodograms contain information about relative site response as well. It is clear from Figures 10 and 11 that the abutment station has larger motions than the downstream station, and that the difference is frequency dependent (considering the acceleration, velocity, and displacement time series to be surrogates for bandpassed ground motions). In sharp contrast are the hodograms for the 1993/01/16 earthquake, shown in Figure 12. Here the motions at the downstream station are larger than for the abutment station for all three types of ground motion. The next section looks at spectral ratios as a more precise way of studying the relative differences in ground motion between the two sites.

The time-alignment of the two horizontal motions is sufficiently accurate that the generally elliptical rather than rectilinear polarization is real, at least for the longer period motions. The elliptical polarization might be evidence of seismic anisotropy (e.g., Zhang and Schwartz, 1994) or could be a result of complex wave interactions due to three-dimenensional variations in seismic propagation velocity.

Comparisons of Spectra

To better study the relative difference of the ground motion at the two sites as a function of frequency, we computed ratios of the smoothed Fourier spectra of the horizontal motions. The results are shown in the right column of graphs in Figure 13. The individual spectra, shown in the left column of graphs in Figure 13, indicate that with a few exceptions peaks in the ratios are not an artifact of holes in the spectra of the denominators. The main exceptions are the large peaks at 4 and 10 Hz for the 1993/01/16 event (bottom of Figure 13). Ratios of response spectra give similar results in the frequency range of dominant motion, but the ratio of Fourier spectra give a better indication of relative motion for frequencies away from the band of most of the ground-motion energy, where the oscillator response can be controlled by frequencies different than the natural frequency of the oscillator. As expected from the hodogram plots, the ratios show the motion at the abutment site to be larger than at the downstream site for the 1989/10/18 and the 1993/08/11 earthquakes. The relative amplifications are not the same for both events, but both show relative peaks in similar frequency ranges: around 1.5 Hz and at frequencies above about 8 Hz. For the 1993/01/16 event, the relative motions are not amplified near 1.5 Hz, and with the exception of the localized peaks near 4 and 10 Hz on the 285 and 195 degree components, which are due to holes in the spectrum of the downstream motion, the ratio at higher frequencies is near or slightly below unity.

Discussion and Conclusions

For most motions recorded at the two sites near Coyote Lake Dam, the abutment station motions are larger than those at the downstream site for a broad range of frequencies. This is not universally the case, however. The fact that the relative difference is not completely consistent for all events, and that the polarizations of the motions can change from one earthquake to another and yet are generally similar for both stations, suggests that complexities due to more than just local site response have an important influence on the motions. These effects can include fault-zone trapped waves (e.g., Spudich and Olsen, 2001; Rovelli *et al.*, 2002; Cultrera *et al.*, 2003, although the fault-zone effects are much more pronounced for the data studied in the latter two papers than those analyzed here) and the apparent attenuation of motion for waves propagating through the fault (e.g., Boore and Hill, 1973). But no single one of these factors can be the reason for the observed

differences in the motion. For example, the waves from the 1989 Loma Prieta earthquake arrive at the sites from a direction almost perpendicular to the Calaveras fault zone, and yet the motions from that earthquake show clear amplification of the abutment station relative to the downstream station; this is unlikely to be due to fault-zone trapped waves.

Because the geology surrounding the downstream site apparently is not nearly as complex as that around the abutment site, and because the station is located on an open slope without a dam or large knob of rock adjacent to the site, it is tempting to consider the motions at the downstream site to be normal. But with data from only two stations it is not possible to say whether the motion at the abutment station is generally amplified or whether motion at the downstream is generally deamplified— either would explain the spectral ratios. Lacking additional, nearby data (something that we hope future researchers will obtain), we attempted to resolve this inherent ambiguity by looking for other sites in a similar site class that recorded the Loma Prieta earthquake at about the same distance. We found two: Anderson Dam downstream and Gilroy 6 (see Figure 1 for locations). The Fourier acceleration spectra from the Anderson Dam and Coyote Lake downstream stations are comparable (Figure 14), while that from Gilroy 6 is significantly below the rest of the spectra (Spudich and Olsen, 2001, have noted that Gilroy 6 is anomalous; they attribute this to the station being in the fault zone, yet actually the station is located on a ridge to the east of the fault zone). The spectrum for the Coyote Lake Dam abutment station is higher than all other spectra. Thus the comparison of spectra in Figure 14 suggests that the Coyote Lake downstream station is "normal". But there is abundant evidence from networks of relatively closely spaced instruments sited in places with what appears to be very uniform geology that ground motions can show significant variations within a distance of 700 m (e.g., Steidl, 1993; Field and Hough, 1997; Baher *et al.*, 2002). In combination with Abrahamson and Darragh's (1985) explanation for the large peak acceleration of 1.29g at the abutment site during the 1984 Morgan Hill earthquake, the uncontroversial peak acceleration of 0.25g at that site from the 1979 Coyote Lake earthquake, and the similarities in particle motion polarizations at both sites for a given event, we cannot make a robust argument that the motions at the abutment site are subject to a strong local site amplification.

Even though we cannot conclusively show that the abutment station has a local site amplification, it is clear that the abutment site is in the midst of very complex geology, with demonstrable rapid lateral variations in geology, and this complexity undoubtedly affects the motions at the site. For this reason we caution against using motions from the site for routine applications based on "normal" sites, such as the derivation of ground-motion prediction equations.

Acknowledgments

We thank Dick Volpe for providing Santa Clara Valley Water District reports and for arranging access to the site, Tom Fumal for sharing reports he had collected describing the geology in the vicinity of the dam, Carl Wentworth for printing out a map of the geology in the area, and Joe Fletcher, Kenichi Kato, Antonio Rovelli, and Chris Stephens for reviewing the paper. The program CoPlot, from www.cohort.com, was very useful in doing some of the data analysis and in creating the line drawings.

References

Abrahamson, N. A. and R. B. Darragh (1985). The Morgan Hill earthquake of April 24, 1984 — The 1.29g acceleration at Coyote Lake Dam: due to directivity, a double event, or both?, *Earthquake Spectra* **1**, 445–455.

Abrahamson, N. A. and W. J. Silva (1997). Empirical response spectral attenuation relations for shallow crustal earthquakes, *Seism. Res. Lett.* **68**, 94–127.

Baher, S., P. M. Davis, and G. Fuis (2002). Separation of site effects and structural focusing in Santa Monica, California: A study of high-frequency weak motions from earthquakes and blasts recorded during the Los Angeles Region Seismic Experiment, *Bull. Seism. Soc. Am.* **92**, 3134–3151.

Bakun, W. H., M. M. Clark, R. S. Cockerham, W. L. Ellsworth, A. G. Lindh, W. H. Prescott, A. F. Shakal, and P. Spudich (1984). The 1984 Morgan Hill, California, earthquake, *Science* **225**, 288–291.

Beroza, G. C. and P. Spudich (1988). Linearized inversion for fault rupture behavior: Application to the 1984 Morgan Hill, California, earthquake, *J. Geophys. Res.* **93**,

6275–6296.

Bonamassa, O. and J. E. Vidale (1991). Directional site resonances observed from aftershocks of the 18 October 1989 Loma Prieta earthquake, *Bull. Seism. Soc. Am.* **81**, 1945–1957.

Boore, D. M. and D. P. Hill (1973). Wave propagation characteristics in the vicinity of the San Andreas fault, in *Proc. Conf. on Tectonic Problems of the San Andreas Fault System*, R. L. Kovach and A. Nur (Editors), School of Earth Sciences, Stanford University, 215–224.

Boore, D. M., W. B. Joyner, and T. E. Fumal (1997). Equations for estimating horizontal response spectra and peak acceleration from western North American earthquakes: A summary of recent work, *Seism. Res. Lett.* **68**, 128–153.

Bouchon, M. (1982). The rupture mechanism of the Coyote Lake earthquake of 6 August 1979 inferred from near-field data, *Bull. Seism. Soc. Am.* **72**, 745–757.

Cultrera, G., A. Rovelli, G. Mele, R. Azzara, A. Caserta, and F. Marra (2003). Azimuth-dependent amplification of weak and strong ground motions within a fault zone (Nocera Umbra, central Italy), *J. Geophys. Res.* **108**, 2156,doi:10.1029/2002JB001929.

Ekström, G. A. (1984). Centroid-moment tensor solution for the April 24, 1984 Morgan Hill, California, earthquake, in *The 1984 Morgan Hill, California Earthquake*, J. H. Bennett and R. W. Sherburne (Editors), Calif. Dept. Conservation, Calif. Div. Mines and Geol. (now Calif. Geological Survey) Special Publication 68, 209–213.

Field, E. H. and S. E. Hough (1997). The variability of PSV response spectra across a dense array deployed during the Northridge aftershock sequence, *Earthquake Spectra* **13**, 243–257.

Fumal, T.E., J.F. Gibbs, and E.F. Roth (1987). Near-surface geology and seismic-wave velocities at six strong-motion stations near Gilroy, California, in *The Morgan Hill, California, Earthquake of April 24, 1984*, Seena N. Hoose (Editor), *U.S. Geological Survey Bulletin* **1639**, 81–88.

Graizer, V., D. Boore, A. Shakal, and J. Tinsley (2002). Unusual strong ground motion amplification at the Coyote Lake Dam, California, *EOS, Trans. Am. Geophys. Union* **83**, Fall Meet. Suppl., Abstract S12B-1208, 2002, p. F1058.

Hartzell, S. H. and T. H. Heaton (1986). Rupture history of the 1984 Morgan Hill, California, earthquake from the inversion of strong motion records, *Bull. Seism. Soc. Am.* **76**, 649–674.

Hovland, H. J., J. C. Gamble, B. J. Mah, and J. E. Valera (1984). The 1984 Morgan Hill earthquake effects near Coyote Dam, in *The 1984 Morgan Hill, California Earthquake*, J. H. Bennett and R. W. Sherburne (Editors), Calif. Dept. Conservation, Calif. Div. Mines and Geol. (now Calif. Geological Survey) Special Publication 68, 71–83.

Liu, H.-L. and D.V. Helmberger (1983). The near-source ground motion of the 6 August 1979 Coyote Lake, California, earthquake, *Bull. Seism. Soc. Am.* **73**, 201–218.

Niazi, M. (1984). Radial asymmetry of the observed PGA and question of focusing in the near-source region of the April 24, 1984 Morgan Hill earthquake, in *The 1984 Morgan Hill, California Earthquake*, J. H. Bennett and R. W. Sherburne (Editors), Calif. Dept. Conservation, Calif. Div. Mines and Geol. (now Calif. Geological Survey) Special Publication 68, 265–271.

Rovelli, A., A. Caserta, F. Marra, and V. Ruggiero (2002). Can seismic waves be trapped inside an inactive fault zone? The case of Nocera Umbra, central Italy, *Bull. Seism. Soc. Am.* **92**, 2217–2232.

Shakal, A. F., R. W. Sherburne, and D. L. Parke (1984a). CDMG strong-motion records from the Morgan Hill, California earthquake of 24 April 1984, *Rep. OSMS 84-07*, Office of Strong Motion Studies, Calif. Div. Mines and Geol. (now Calif. Geological Survey), 101 pp.

Shakal, A. F., R. W. Sherburne, and D. L. Parke (1984b). Principal features of the strong-motion data from the 1984 Morgan Hill earthquake, in *The 1984 Morgan Hill, California Earthquake*, J. H. Bennett and R. W. Sherburne (Editors), Calif. Dept. Conservation, Calif. Div. Mines and Geol. (now Calif. Geological Survey) Special Publication 68, 249–264.

Spudich, P. and K.B. Olsen (2001). Fault zone amplified waves as a possible seismic hazard along the Calaveras fault in central California, *Geophys. Res. Lett.* **28**, 2533–2536.

Spudich, P., M. Hellweg, and W. H. K. Lee (1996). Directional topographic site response at Tarzana observed in aftershocks of the 1994 Northridge, California, earthquake: Implications for the mainshock motions, *Bull. Seism. Soc. Am.* **86**, S193–S208.

Steidl, J. H. (1993). Variation of site response at the UCSB dense array of portable accelerometers, *Earthquake Spectra* **9**, 289–302.

Tepel, R.E. (1984). Evaluation of the effects of the Morgan Hill earthquake of April 24, 1984 at Coyote dam and spillway, *San Jose, Calif., Santa Clara Valley Water District report*, 45 p.

Tepel, R. E., R. L. Volpe, and G. Bureau (1984). Performance of Anderson and Coyote Dams during the Morgan Hill earthquake of 24 April 1984, in *The 1984 Morgan Hill, California Earthquake*, J. H. Bennett and R. W. Sherburne (Editors), Calif. Dept. Conservation, Calif. Div. Mines and Geol. (now Calif. Geological Survey) Special Publication 68, 53–70.

Uhrhammer, R. A. and R. B. Darragh (1984). The Halls Valley ("Morgan Hill") earthquake sequence April 24 through June 30, in *The 1984 Morgan Hill, California Earthquake*, J. H. Bennett and R. W. Sherburne (Editors), Calif. Div. Mines and Geol. (now Calif. Geological Survey) Special Publication 68, 191–208.

Vidale, J. E., O. Bonamassa, and H. Houston (1991). Directional site resonances observed from the 1 October 1987 Whittier Narrows, California, earthquake and the 4 October aftershock, *Earthquake Spectra* **7**, 107–125.

Wentworth, C.M., M.C. Blake, Jr., R.J. McLaughlin, and R.W. Graymer (1998). Preliminary geologic map of the San Jose 30 X 60-minute quadrangle, California; a digital database, *U.S. Geol. Surv. Open-File Rept. OF 98-0795*, 14 p. Available on the web at http://wrgis.wr.usgs.gov/open-file/of98-795.

Zhang, Z. and S. Y. Schwartz (1994). Seismic anisotropy in the shallow crust of the Loma Prieta segment of the San Andreas fault system, *J. Geophys. Res.* **99**, 9651–9661.

U.S. Geological Survey, MS 977
345 Middlefield Road
Menlo Park, California 94025
boore@usgs.gov
jtinsley@usgs.gov
(D.M.B., J.C.T.)

California Geological Survey
Strong Motion Instrumentation Program
801 K Street
Sacramento, California 95814
vgraizer@consrv.ca.gov
tshakal@consrv.ca.gov
(V.M.G, A.F.S.)

Table 1. Station information (coordinates from GPS instrument, using NAD83 datum).

Station Name	Latitude (°N)	Longitude (°E)
Coyote Lake Dam: Abutment	37.11818	−121.55112
Coyote Lake Dam: Downstream	37.12442	−121.55197

Table 2. Earthquake information.

						Epicenter		Peak Acceleration (g)				
Date*	T(GMT)	Lat(°N)	Long(°E)	D(km)	M†	R_{ep} (km)	Az (°)	Comp‡	Abut	Down	Ratio	Dig?
1979/08/06	17:05:23	37.104	-121.513	9	5.7	4	295	285	0.25	–	–	Y
1984/04/24	21:15:19	37.310	-121.679	9	6.2	24	152	285	1.29	–	–	Y
1989/10/18	00:04:15	37.036	-121.880	17	6.9	31	73	285	0.49	0.19	2.6	Y
1993/01/16	06:29:35	37.018	-121.463	8	5.1	14	325	195	0.19	0.27	0.7	Y
1993/08/11	22:33:04	37.312	-121.679	9	5.0	24	151	195	0.08	0.05	1.5	Y
1995/09/13	20:36:47	37.096	-121.512	8	4.3	4	310	285	0.07	0.05	1.5	N
2002/05/14	05:00:30	36.967	-121.600	8	4.9	18	15	285	0.04	0.03	1.3	N

* Meaning of column headings: "Date", "T", "Lat", "Long", "D", "M", "r_{ep}", "Az", "Comp", "Abut", "Down", "Ratio", "Dig?" = earthquake date, origin time, epicentral location (latitude and longitude), hypocentral depth, moment magnitude, epicentral distance, epicenter-to-station azimuth, component of the motion containing the peak acceleration, the peak acceleration at the abutment and the downstream stations, the ratio of peak accelerations at the two stations, and a flag to indicate if recordings of the earthquake have been digitized.

† Moment magnitude: values for events up to 1989 from http://www.seismology.harvard.edu/CMTsearch.html; values for events after 1989 from link on http://www.seismo.berkeley.edu/∼dreger/mtindex.html

‡ The peak acceleration is on the same component for both stations

Figure Captions

Figure 1. Location of the earthquakes recorded at the Coyote Lake Dam stations. The Coyote Lake Dam stations are shown by large triangles; the small triangles are other stations discussed in the paper. The surface projection of a rectangle approximating the rupture surface (after Spudich and Olsen, 2001) is shown for the 1979 Coyote Lake (CL79=1979/08/06), 1984 Morgan Hill (MH84=1984/04/24), and 1989 Loma Prieta (LP89=1989/10/18) earthquakes; the epicenters for these three events are shown by open circles. The epicenters of the other events are shown by stars. All events were recorded at the abutment station, and all but the 1979 and 1984 events were recorded at the downstream station. The events 1995/09/13 and 2002/05/14 produced records too small to be digitized; only the peak accelerations for those events are used in this paper.

Figure 2. Acceleration, velocity, and displacement time series for the two horizontal components of motion from the 1984 Morgan Hill earthquake, recorded at the Coyote Lake abutment station. Note the large pulse of acceleration on the 285 degree component. The component directions are in degrees clockwise from north. The acceleration traces are unfiltered; the velocity and displacement traces were obtained by integration of filtered acceleration traces. The acceleration traces for both components were padded with 13 sec of zeros before and after the motion and were filtered using a zero-phase Butterworth low-cut filter with corner frequency of 0.12 Hz. The order of the filter was chosen so that its response goes as f^4 for low frequencies. The large pre-S motion in the displacement traces is a consequence of the interaction of the acausal filter response and the large peak in acceleration; it cannot be reduced by tapering of the motions near the start of the record. The only way of reducing its effect is to choose a higher low-cut frequency.

Figure 3. Pictures showing the two sites. top left: looking across dam crest at abutment site (in small shed to the left of the large knob-like rock outcrop; the shed is within about one meter of the outcrop); bottom left: looking up the downstream face of the dam toward the abutment station (left of the large knob of rock); top right: walking up 10 degree slope toward the downstream site; bottom right: the downstream site— notice boulder float on ground surface.

Figure 4. Topographic map in vicinity of Coyote Lake Dam, showing the locations of the abutment and downstream stations.

Figure 5. "As-constructed drawing" from Tepel (1984), showing pre-dam (dashed where under present day topography) and post-dam (solid) contours (contour interval is 5 feet). The parallel set of contours show the upstream and downstream faces of the dam. The downstream face slopes toward the top of the figure.

Figure 6. Acceleration, velocity, and displacement time series from the 1989 Loma Prieta earthquake, recorded at the abutment and downstream stations. The traces have been aligned to start at the same absolute time (00:04:24.6 GMT). Shown is the horizontal motion rotated into a direction corresponding to the peak polarization determined from the velocity traces. Note that the time-axis scaling is different for the acceleration, velocity, and displacement traces. This was done to make it easier to compare the abutment and downstream motions. For the displacements, the motions at the two stations are very similar, but at higher frequencies (as shown in the velocity and acceleration traces) the correlation starts to break down after the first arrival, and the abutment station motion is generally larger than the downstream station motion.

Figure 7. Acceleration, velocity, and displacement time series from the 1993/01/16 earthquake, recorded at the abutment and downstream stations. Shown is the horizontal motion rotated into a direction normal (56°) and parallel (326°) to the fault strike. Absolute time was not available for the record. The polarization for this event is dominated by fault-normal motion, unlike the motion from earlier events, and the motion is generally larger on the downstream site than on the abutment site, again unlike the previously shown events.

Figure 8. Acceleration, velocity, and displacement time series from the 1993/08/11 earthquake, recorded at the abutment and downstream stations. Shown is the horizontal motion rotated into a direction normal (56°) and parallel (326°) to the fault strike. Absolute time was not available for the record.

Figure 9. Hodograms of 3 sec of motion windowing the largest accelerations for the horizontal components of motion at the abutment station for the 1979 Coyote Lake and the 1984 Morgan Hill earthquakes. The hodograms are plotted for a time window from 10–13 sec and 15–18 sec for the 1979 and the 1984 records, respectively, relative to the trigger time of the records (as distributed by the Strong Motion Instrumentation Program of the California Geological Survey). Hodograms are shown for ground acceleration, velocity, and

displacement. The radial gray lines are drawn every 10 degrees, with heavier lines every 30 degrees, to aid in determining orientations. The heavy diagonal line shows the local orientation of the Calaveras fault, as determined from maps and accounting for right-step in the San Felipe valley. North and east are up and to the right. The accelerations for both components from the 1979 and 1984 earthquakes were low-cut filtered at 0.25 Hz and 0.12 Hz, respectively, with a zero-phase Butterworth filter as described in the caption to Figure 2. (In constructing the hodogram for the 1979 Coyote Lake earthquake, the corrected horizontal orientations of 285 and 195 degrees, as noted by Shakal *et al.* (1984b), were used.)

Figure 10. Hodograms of 4 sec of motion windowing the largest accelerations for the horizontal components of motion for the 1989 Loma Prieta earthquake, at the abutment and the downstream sites. The hodograms are plotted for a time window from 4–8 sec relative to the trigger time of the records (as distributed by the Strong Motion Instrumentation Program of the California Geological Survey). Plot labeling as in Figure 9, except the records are for recordings of the same earthquake (1989 Loma Prieta) at the two stations. The accelerograms for both stations and both components were low-cut and high-cut filtered using ramps between 0.08 and 0.16 Hz and between 23 Hz and 25 Hz, respectively. The jaggedness of the acceleration hodograms is probably a result of relatively high-frequency content and a low sampling rate of 50 samples per second.

Figure 11. Hodograms of the horizontal components of motion for the 1993/01/16 earthquake, at the abutment and the downstream sites. Plot labeling as in Figure 9, except the records are for recordings of the same earthquake (1993/01/16) at the two stations. The thin and thick lines indicate time segments of 2.0–3.5 and 3.5–5.0 sec, respectively. The first window was chosen so as to contain the maximum accelerations (see Figure 7). The accelerograms for both stations and both components were low-cut and high-cut filtered using ramps between 0.3 and 0.6 Hz and between 23 Hz and 25 Hz, respectively.

Figure 12. Hodograms of the horizontal components of motion for the 1993/08/11 earthquake, at the abutment and the downstream sites. Plot labeling as in Figure 9, except the records are for recordings of the same earthquake (1993/08/11) at the two stations. The thin and thick lines indicate time segments of 3.0–5.0 and 5.0–7.0 sec, respectively. The first window was chosen so as to contain the maximum accelerations

(see Figure 8). The accelerograms for both stations and both components were low-cut and high-cut filtered using ramps between 0.4 and 0.8 Hz and between 23 Hz and 25 Hz, respectively.

Figure 13. Fourier spectra (left column of graphs) and spectral ratios (righ column of graphs) of the three events recorded at both the abutment and downstream stations for which the analog records were large enough to be digitized. The spectra for the frequency range shown are judged to be well above the noise. The spectra of the two stations have been smoothed using a triangular smoothing function with half-width of 1 Hz before forming the ratio. The Fourier spectra are plotted using logarithmic scaling for the ordinate to allow the reader to judge the spectral ratios shown in the right column of graphs.

Figure 14. Fourier acceleration spectra for four recordings of the 1989 Loma Prieta earthquake at somewhat comparable distances from the surface projection of the fault rupture: Anderson Dam downstream (18.0 km), Coyote Lake Dam downstream (19.0), Gilroy 6 (17.0), and for comparison, Coyote Lake Dam abutment (18.5) (see Figure 1 for station locations). Corrections for geometric spreading were not applied; they are less than a factor of 0.92 (the factor to go from Gilroy 6 to Coyote Lake downstream). Except for Anderson Dam downstream the spectra are shown for the fault parallel component; for Anderson Dam downstream particle motion plots show elliptical polarization, which is probably due to the two traces not being precisely aligned in time when digitized; fortunately, the as-recorded component of 333° is close to the fault parallel direction. Both Gilroy 6 and Coyote Lake Dam downstream are slightly to the east of the Calaveras fault zone; Anderson Dam downstream is to the west of the fault zone. Both the Anderson Dam and the Gilroy 6 sites fall into NEHRP class C, with average shear wave velocities to 30 m of 489 m/sec and 589 m/sec, respectively. The velocities at the Coyote Lake Dam sites have not been measured, but it is likely that the sites would fall into the NEHRP class C category ($360\,\mathrm{m/sec} < \bar{V}_s(30m) \leq 760\,\mathrm{m/sec}$).

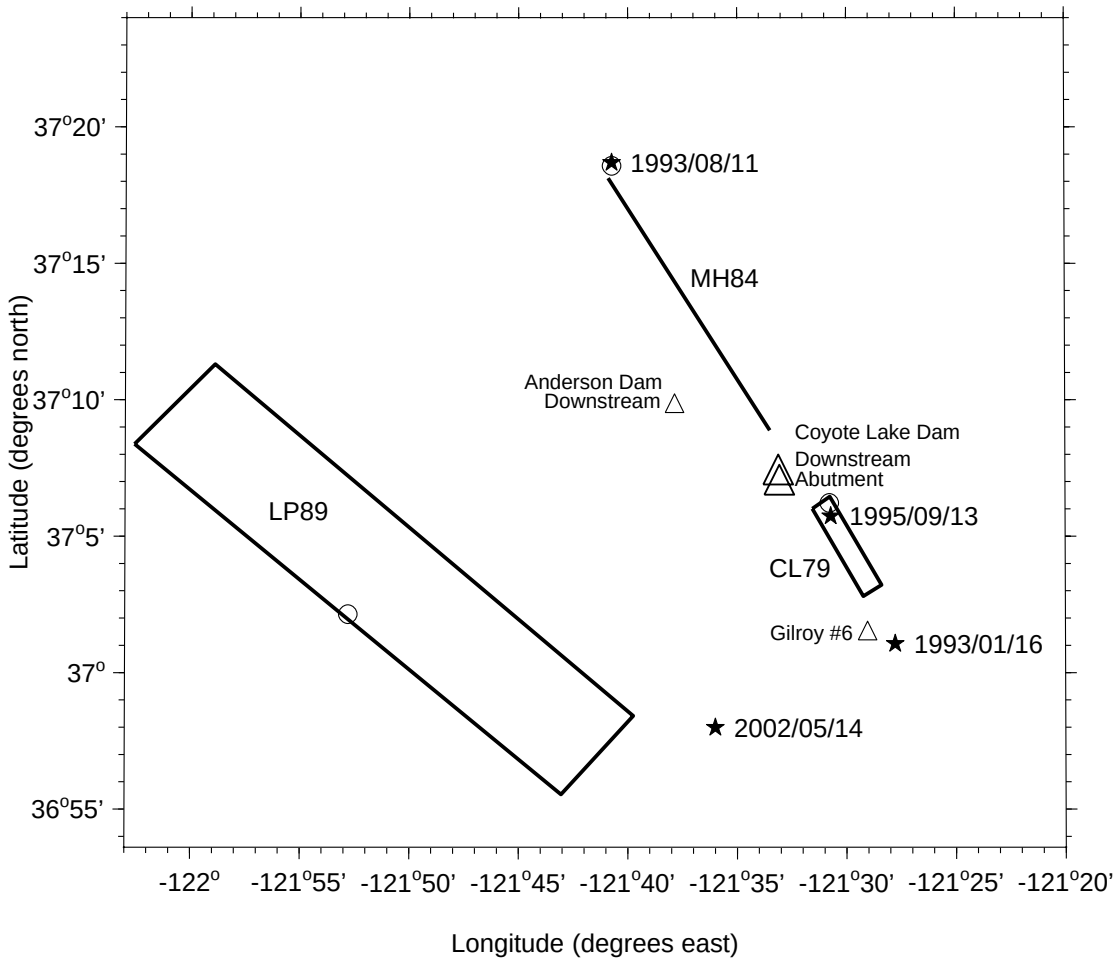

Figure 1. Location of the earthquakes recorded at the Coyote Lake Dam stations. The Coyote Lake Dam stations are shown by large triangles; the small triangles are other stations discussed in the paper. The surface projection of a rectangle approximating the rupture surface (after Spudich and Olsen, 2001) is shown for the 1979 Coyote Lake (CL79=1979/08/06), 1984 Morgan Hill (MH84=1984/04/24), and 1989 Loma Prieta (LP89=1989/10/18) earthquakes; the epicenters for these three events are shown by open circles. The epicenters of the other events are shown by stars. All events were recorded at the abutment station, and all but the 1979 and 1984 events were recorded at the downstream station. The events 1995/09/13 and 2002/05/14 produced records too small to be digitized; only the peak accelerations for those events are used in this paper.

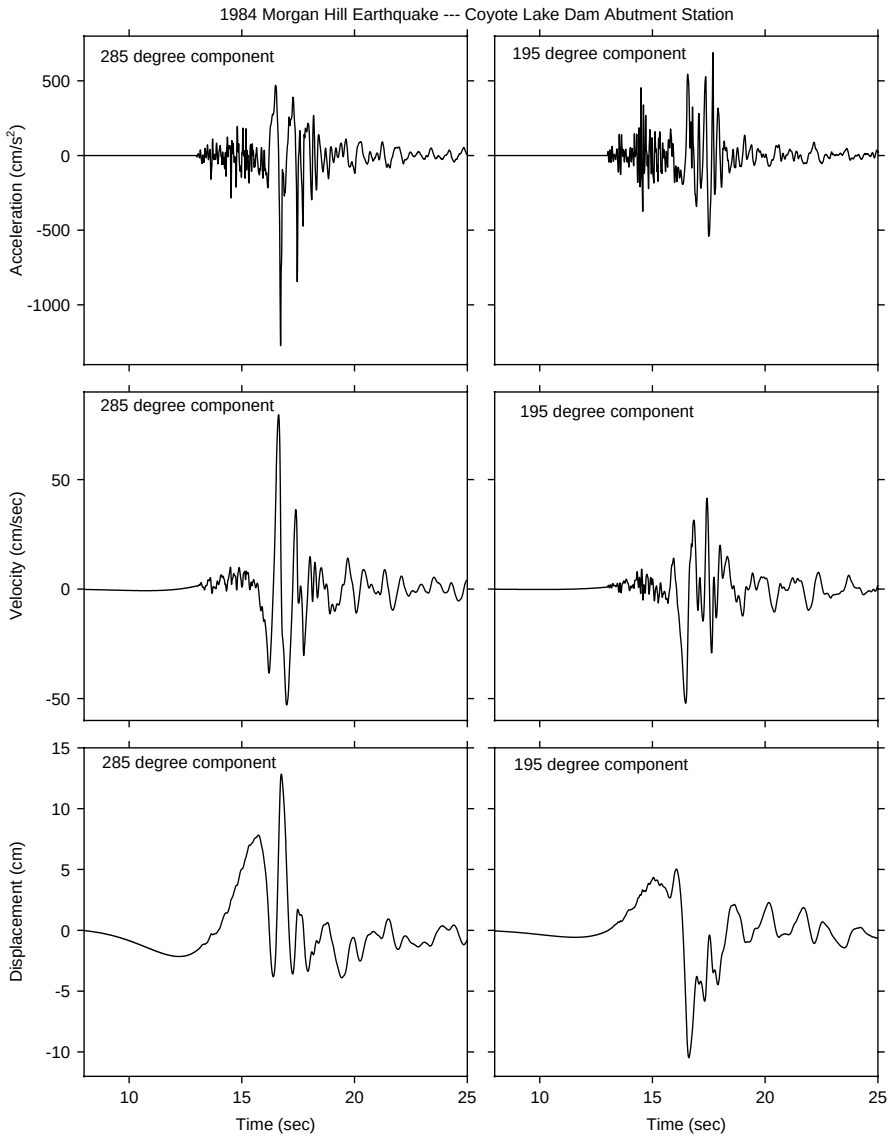

Figure 2. Acceleration, velocity, and displacement time series for the two horizontal components of motion from the 1984 Morgan Hill earthquake, recorded at the Coyote Lake abutment station. Note the large pulse of acceleration on the 285 degree component. The component directions are in degrees clockwise from north. The acceleration traces are unfiltered; the velocity and displacement traces were obtained by integration of filtered acceleration traces. The acceleration traces for both components were padded with 13 sec of zeros before and after the motion and were filtered using a zero-phase Butterworth low-cut filter with corner frequency of 0.12 Hz. The order of the filter was chosen so that its response goes as f^4 for low frequencies. The large pre-S motion in the displacement traces is a consequence of the interaction of the acausal filter response and the large peak in acceleration; it cannot be reduced by tapering of the motions near the start of the record. The only way of reducing its effect is to choose a higher low-cut frequency.

Figure 3. Pictures showing the two sites. top left: looking across dam crest at abutment site (in small shed to the left of the large knob-like rock outcrop; the shed is within about one meter of the outcrop); bottom left: looking up the downstream face of the dam toward the abutment station (left of the large knob of rock); top right: walking up 10 degree slope toward the downstream site; bottom right: the downstream site— notice boulder float on ground surface.

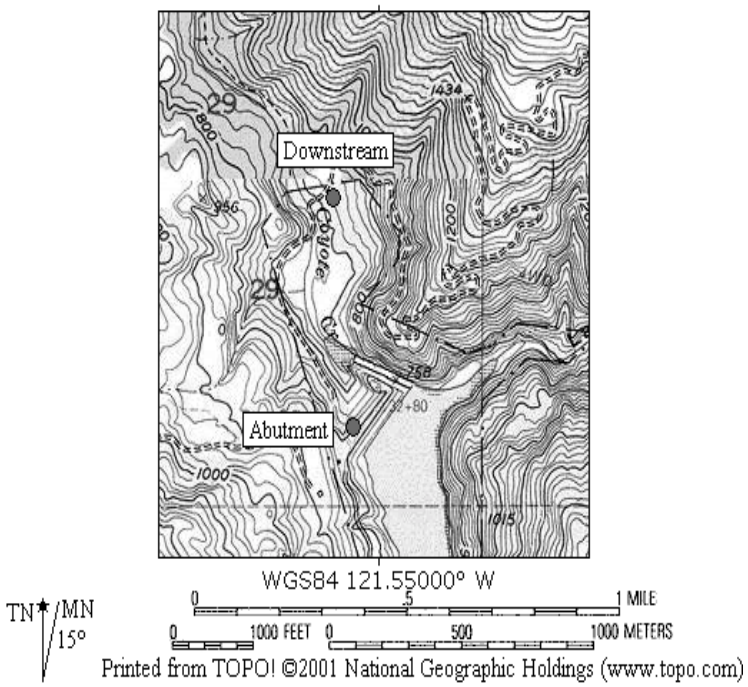

Figure 4. Topographic map in vicinity of Coyote Lake Dam, showing the locations of the abutment and downstream stations.

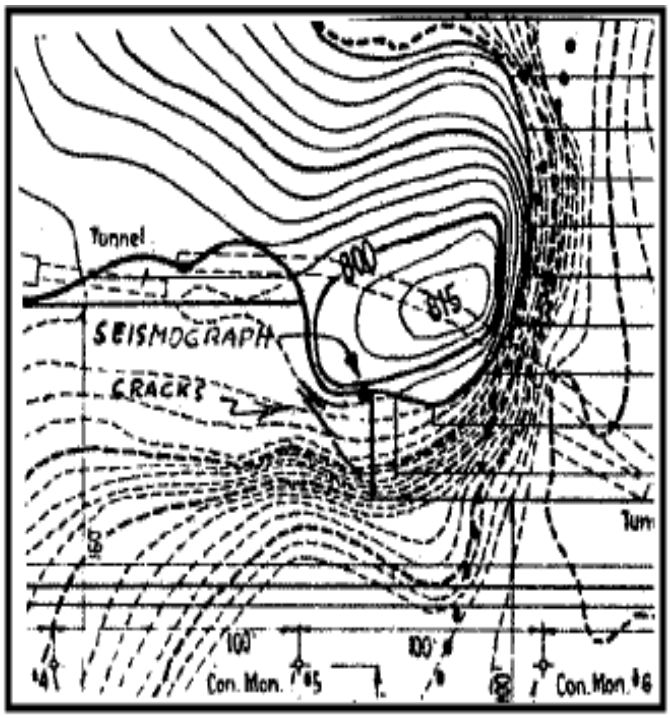

Figure 5. "As-constructed drawing" from Tepel (1984), showing pre-dam (dashed where under present day topography) and post-dam (solid) contours (contour interval is 5 feet). The parallel set of contours show the upstream and downstream faces of the dam. The downstream face slopes toward the top of the figure.

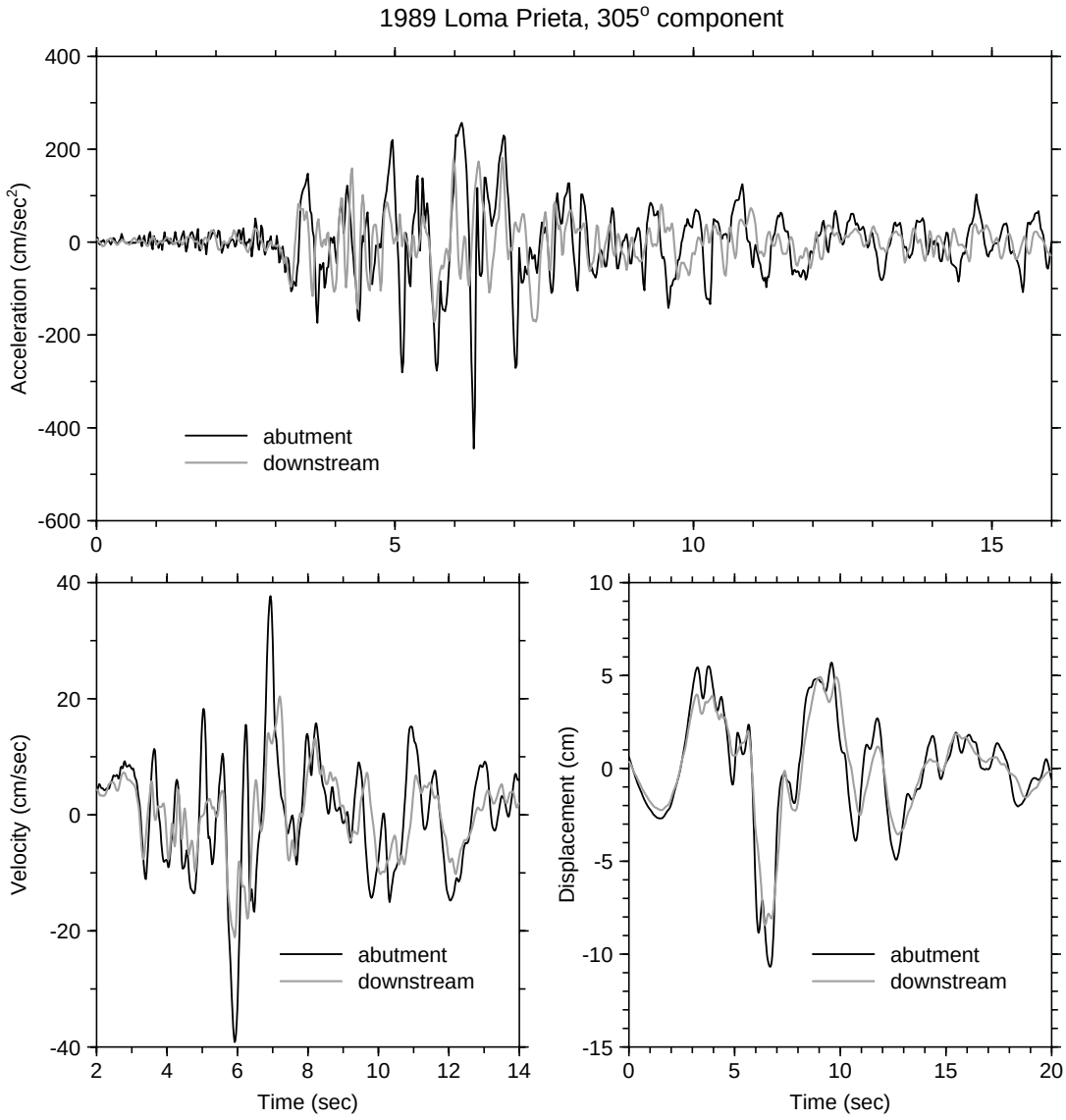

Figure 6. Acceleration, velocity, and displacement time series from the 1989 Loma Prieta earthquake, recorded at the abutment and downstream stations. The traces have been aligned to start at the same absolute time (00:04:24.6 GMT). Shown is the horizontal motion rotated into a direction corresponding to the peak polarization determined from the velocity traces. Note that the time-axis scaling is different for the acceleration, velocity, and displacement traces. This was done to make it easier to compare the abutment and downstream motions. For the displacements, the motions at the two stations are very similar, but at higher frequencies (as shown in the velocity and acceleration traces) the correlation starts to break down after the first arrival, and the abutment station motion is generally larger than the downstream station motion.

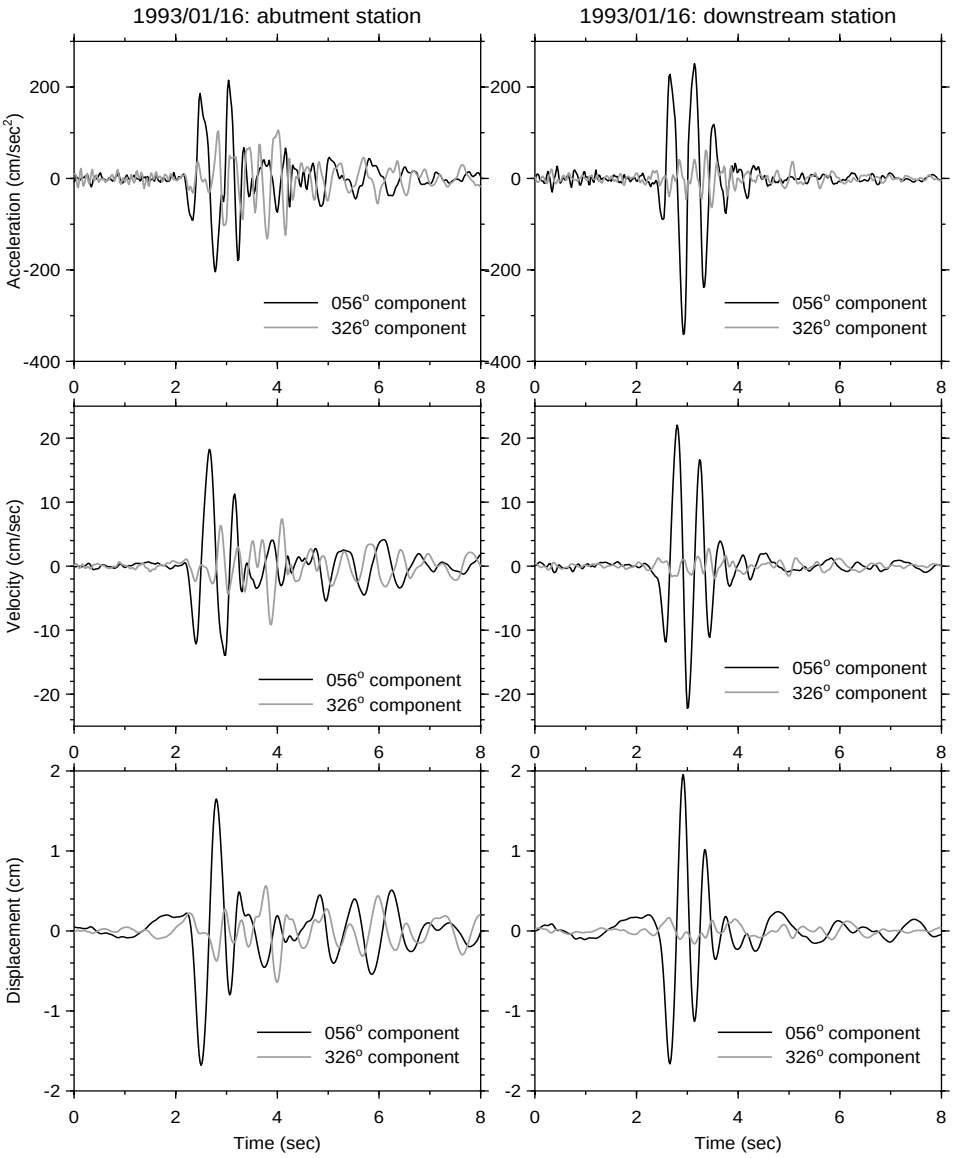

Figure 7. Acceleration, velocity, and displacement time series from the 1993/01/16 earthquake, recorded at the abutment and downstream stations. Shown is the horizontal motion rotated into a direction normal (56°) and parallel (326°) to the fault strike. Absolute time was not available for the record. The polarization for this event is dominated by fault-normal motion, unlike the motion from earlier events, and the motion is generally larger on the downstream site than on the abutment site, again unlike the previously shown events.

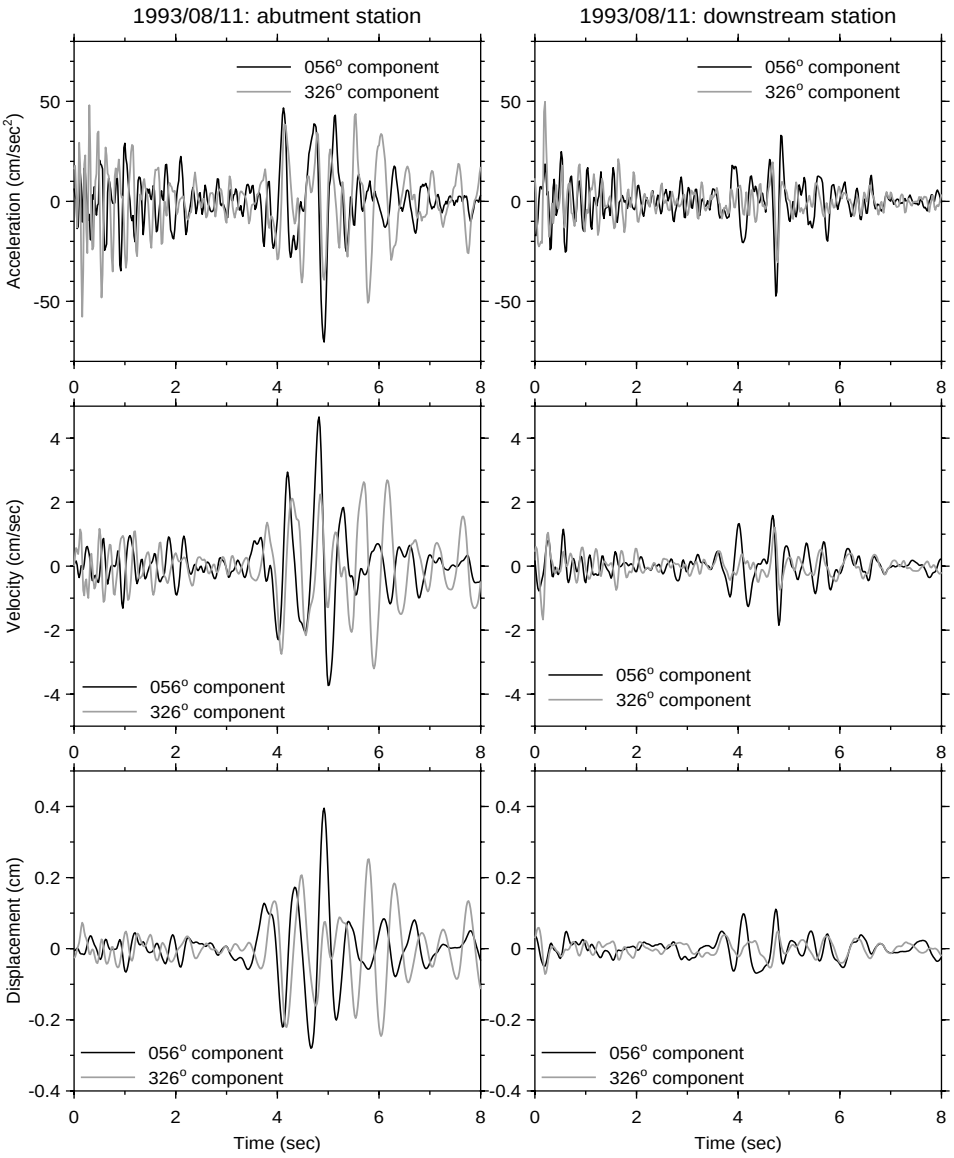

Figure 8. Acceleration, velocity, and displacement time series from the 1993/08/11 earthquake, recorded at the abutment and downstream stations. Shown is the horizontal motion rotated into a direction normal (56°) and parallel (326°) to the fault strike. Absolute time was not available for the record.

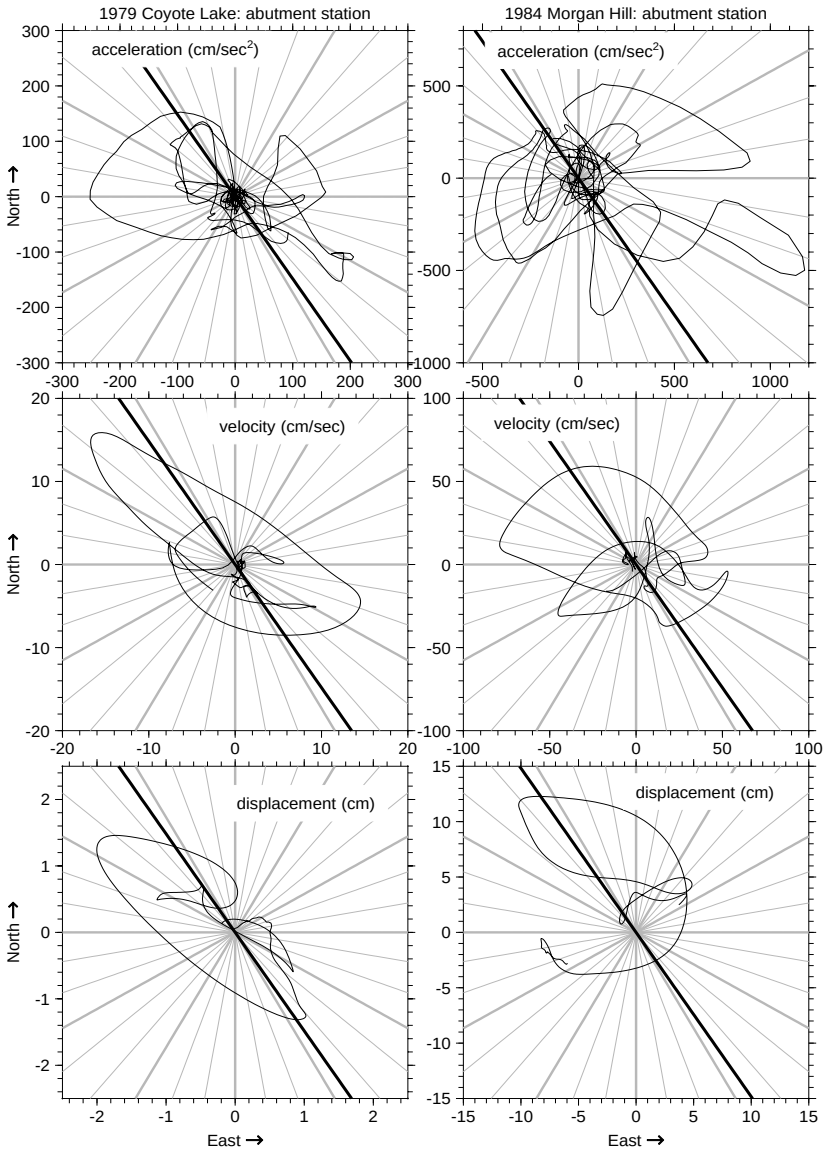

Figure 9. Hodograms of 3 sec of motion windowing the largest accelerations for the horizontal components of motion at the abutment station for the 1979 Coyote Lake and the 1984 Morgan Hill earthquakes. The hodograms are plotted for a time window from 10–13 sec and 15–18 sec for the 1979 and the 1984 records, respectively, relative to the trigger time of the records (as distributed by the Strong Motion Instrumentation Program of the California Geological Survey). Hodograms are shown for ground acceleration, velocity, and displacement. The radial gray lines are drawn every 10 degrees, with heavier lines every 30 degrees, to aid in determining orientations. The heavy diagonal line shows the local orientation of the Calaveras fault, as determined from maps and accounting for right-step in the San Felipe valley. North and east are up and to the right. The accelerations for both components from the 1979 and 1984 earthquakes were low-cut filtered at 0.25 Hz and 0.12 Hz, respectively, with a zero-phase Butterworth filter as described in the caption to Figure 2. (In constructing the hodogram for the 1979 Coyote Lake earthquake, the corrected horizontal orientations of 285 and 195 degrees, as noted by Shakal *et al.* (1984b), were used.)

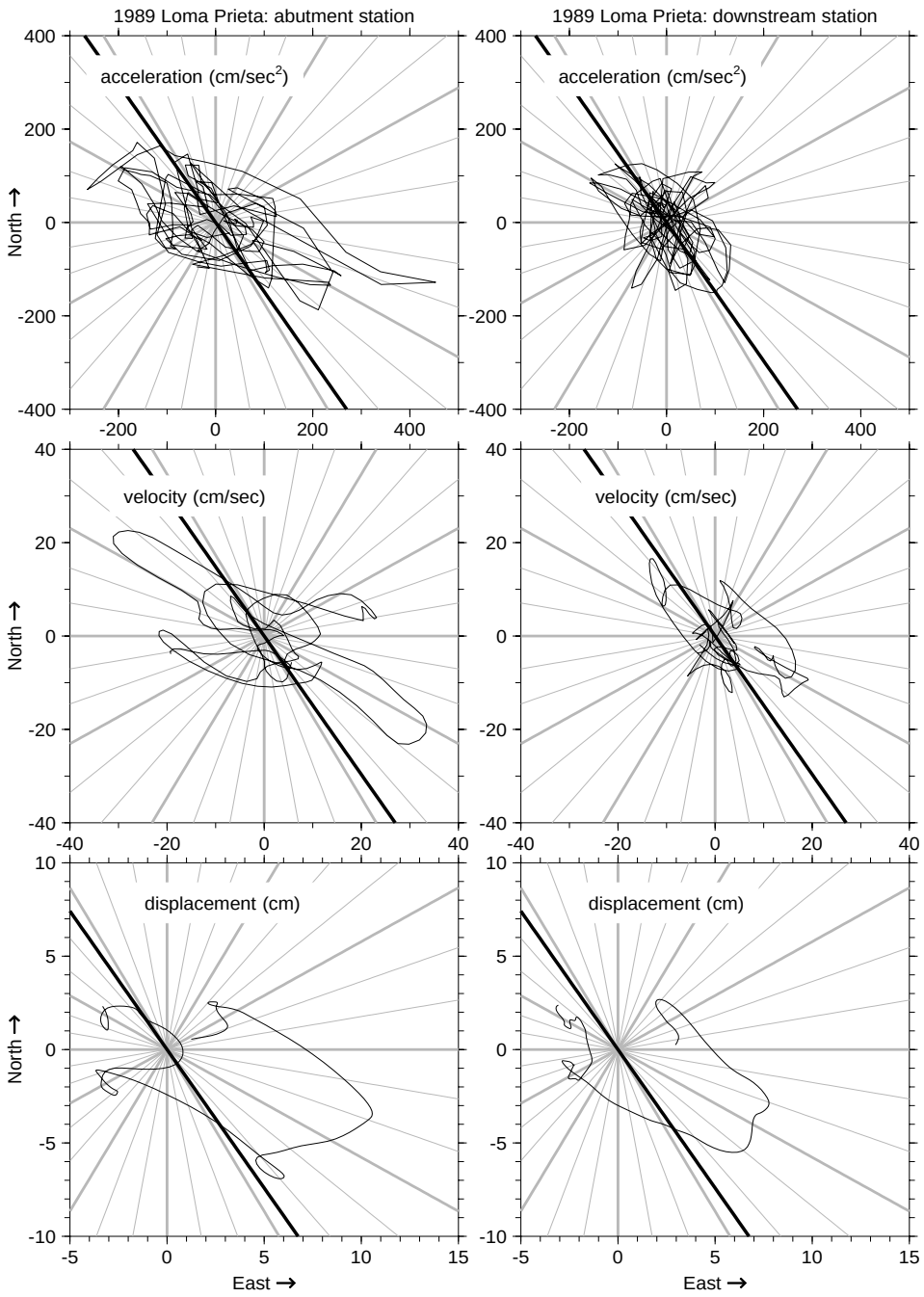

Figure 10. Hodograms of 4 sec of motion windowing the largest accelerations for the horizontal components of motion for the 1989 Loma Prieta earthquake, at the abutment and the downstream sites. The hodograms are plotted for a time window from 4–8 sec relative to the trigger time of the records (as distributed by the Strong Motion Instrumentation Program of the California Geological Survey). Plot labeling as in Figure 9, except the records are for recordings of the same earthquake (1989 Loma Prieta) at the two stations. The accelerograms for both stations and both components were low-cut and high-cut filtered using ramps between 0.08 and 0.16 Hz and between 23 Hz and 25 Hz, respectively. The jaggedness of the acceleration hodograms is probably a result of relatively high-frequency content and a low sampling rate of 50 samples per second.

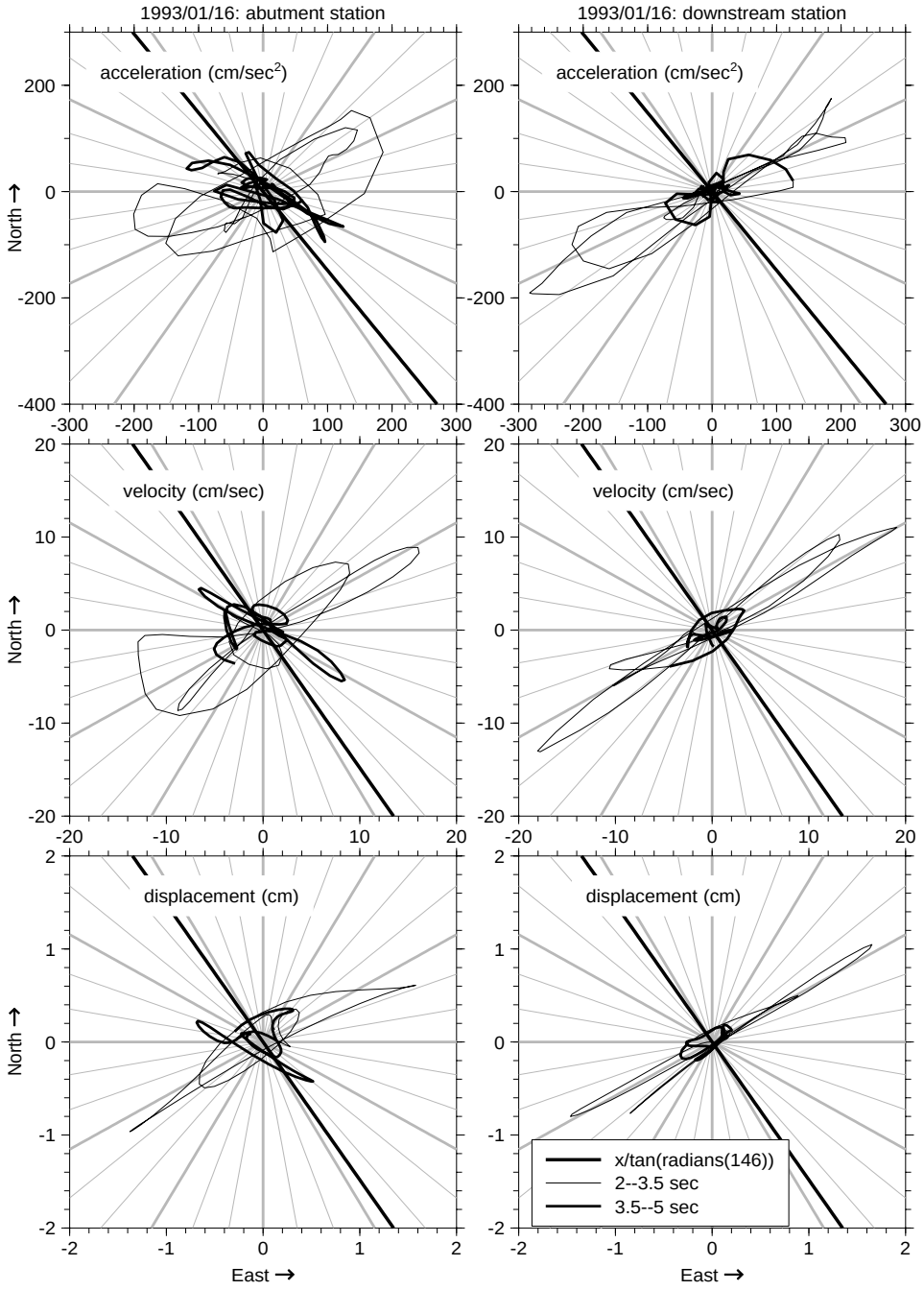

Figure 11. Hodograms of the horizontal components of motion for the 1993/01/16 earthquake, at the abutment and the downstream sites. Plot labeling as in Figure 9, except the records are for recordings of the same earthquake (1993/01/16) at the two stations. The thin and thick lines indicate time segments of 2.0–3.5 and 3.5–5.0 sec, respectively. The first window was chosen so as to contain the maximum accelerations (see Figure 7). The accelerograms for both stations and both components were low-cut and high-cut filtered using ramps between 0.3 and 0.6 Hz and between 23 Hz and 25 Hz, respectively.

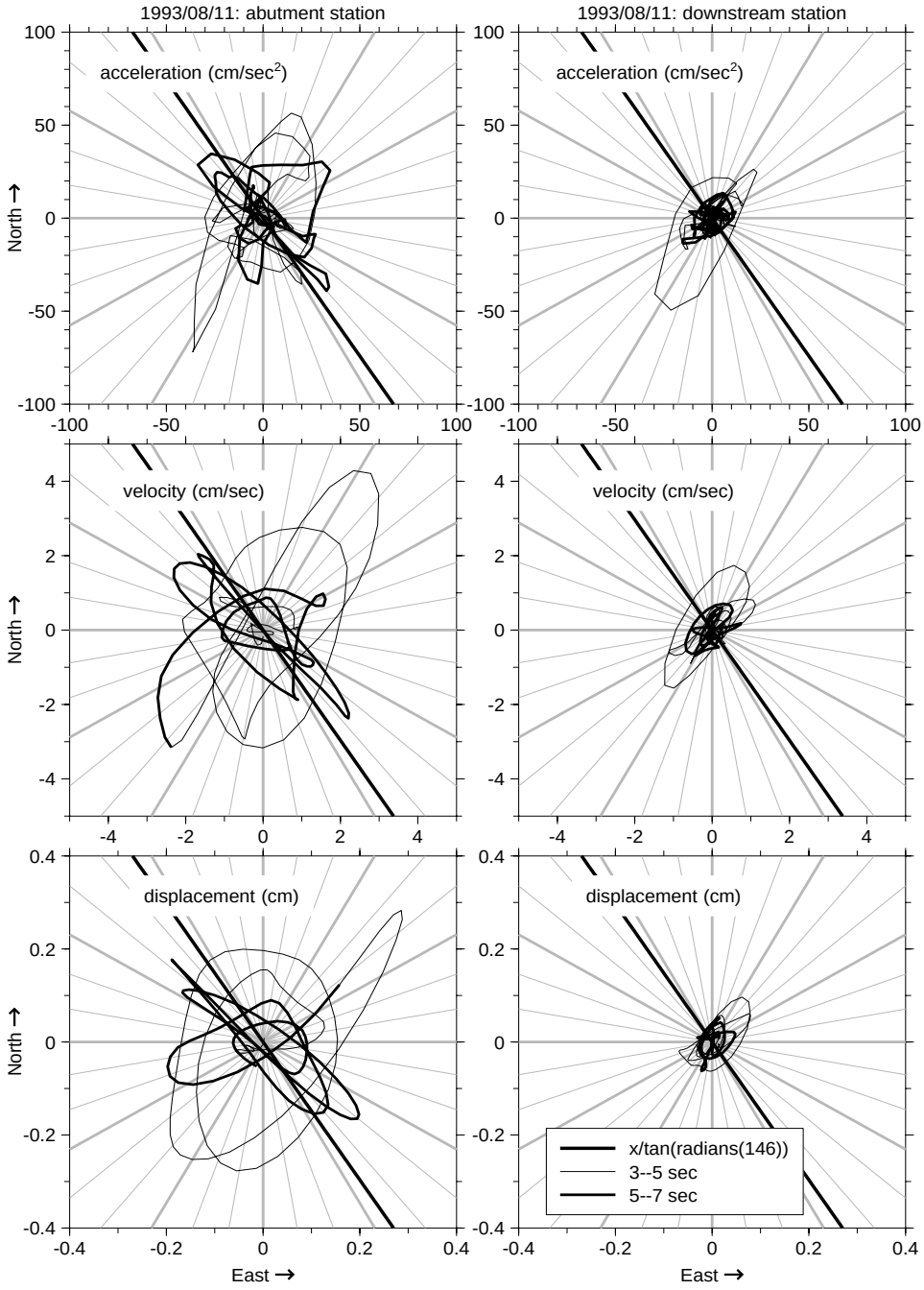

Figure 12. Hodograms of the horizontal components of motion for the 1993/08/11 earthquake, at the abutment and the downstream sites. Plot labeling as in Figure 9, except the records are for recordings of the same earthquake (1993/08/11) at the two stations. The thin and thick lines indicate time segments of 3.0–5.0 and 5.0–7.0 sec, respectively. The first window was chosen so as to contain the maximum accelerations (see Figure 8). The accelerograms for both stations and both components were low-cut and high-cut filtered using ramps between 0.4 and 0.8 Hz and between 23 Hz and 25 Hz, respectively.

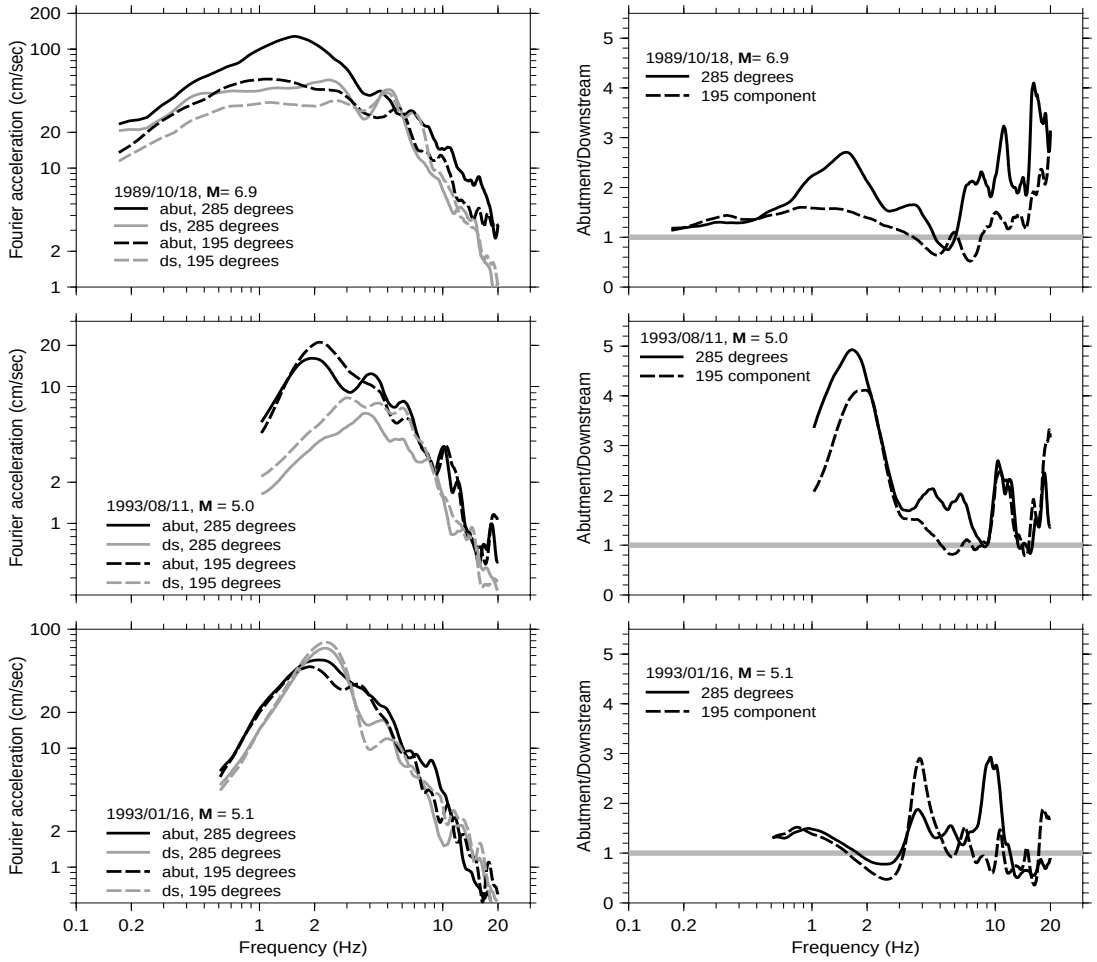

Figure 13. Fourier spectra (left column of graphs) and spectral ratios (righ column of graphs) of the three events recorded at both the abutment and downstream stations for which the analog records were large enough to be digitized. The spectra for the frequency range shown are judged to be well above the noise. The spectra of the two stations have been smoothed using a triangular smoothing function with half-width of 1 Hz before forming the ratio. The Fourier spectra are plotted using logarithmic scaling for the ordinate to allow the reader to judge the spectral ratios shown in the right column of graphs.

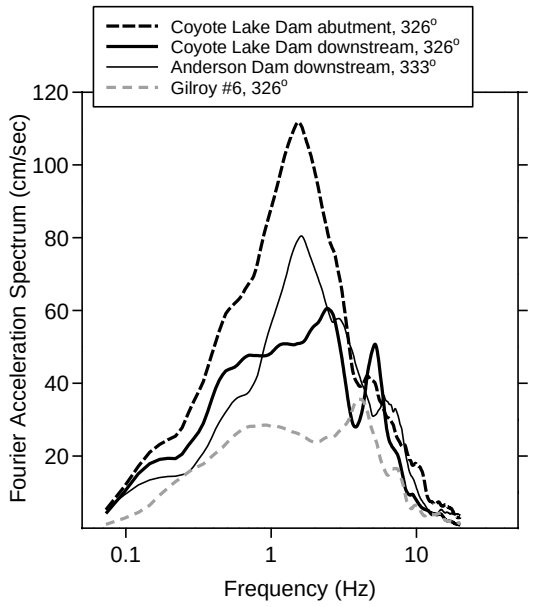

Figure 14. Fourier acceleration spectra for four recordings of the 1989 Loma Prieta earthquake at somewhat comparable distances from the surface projection of the fault rupture: Anderson Dam downstream (18.0 km), Coyote Lake Dam downstream (19.0), Gilroy 6 (17.0), and for comparison, Coyote Lake Dam abutment (18.5) (see Figure 1 for station locations). Corrections for geometric spreading were not applied; they are less than a factor of 0.92 (the factor to go from Gilroy 6 to Coyote Lake downstream). Except for Anderson Dam downstream the spectra are shown for the fault parallel component; for Anderson Dam downstream particle motion plots show elliptical polarization, which is probably due to the two traces not being precisely aligned in time when digitized; fortunately, the as-recorded component of 333° is close to the fault parallel direction. Both Gilroy 6 and Coyote Lake Dam downstream are slightly to the east of the Calaveras fault zone; Anderson Dam downstream is to the west of the fault zone. Both the Anderson Dam and the Gilroy 6 sites fall into NEHRP class C, with average shear wave velocities to 30 m of 489 m/sec and 589 m/sec, respectively. The velocities at the Coyote Lake Dam sites have not been measured, but it is likely that the sites would fall into the NEHRP class C category ($360\,\mathrm{m/sec} < \bar{V}_s(30m) \leq 760\,\mathrm{m/sec}$).